

Detoxification of Cr(VI) using biochar-supported Cu/Fe bimetallic nanoparticles

Fengli Shao, Shaoyu Zhou, Jiaxin Xu, Qiong Du, Jianqiu Chen*, Jingge Shang*

School of Engineering, China Pharmaceutical University, #639 Longmian Avenue, Nanjing 211198, China, Tel./Fax: +86 25 86185190; emails: cjqr@163.com, 1020060993@cpu.edu.cn (J. Chen), shangjingge@gmail.com, gege@cpu.edu.cn (J. Shang), fengli.shao@stu.cpu.edu.cn (F. Shao), 3456600851@qq.com (S. Zhou), 1241024923@qq.com (J. Xu), duqiong116@163.com (Q. Du)

Received 17 September 2018; Accepted 27 March 2019

ABSTRACT

Nanoscale zero-valent iron (nZVI) has been proven to be more effective for the treatment of hexavalent chromium (Cr(VI)) when modified with the transition metal Cu. In this study, biochar-supported Cu/Fe bimetallic nanoparticles (Cu-nZVI/BC) were prepared and used for Cr(VI) removal from aqueous solution. The effects of the pH value, the initial concentration of Cr(VI), coexisting ions and humic acids (HA) were investigated. The compositional structures of Cu-nZVI/BC were analyzed by transmission electron microscopy, scanning electron microscopy, X-ray diffraction and X-ray photoelectron spectroscopy. The maximum removal efficiency of Cr(VI) was 50.57% ($126.41 \pm 3.75 \text{ mg g}^{-1}$) for Cu-nZVI/BC at pH 2. The adsorption kinetic data were in agreement with the pseudo-second-order model, which confirmed that the adsorption step was a chemical adsorption and reduction process. The presence of Ca^{2+} and NO_3^- had an inhibitory effect on Cr(VI) removal, while dHA increased the removal efficiency at high concentrations. This study proves that Cu-nZVI/BC removal of solution Cr(VI) is feasible and shows significant potential in practical applications.

Keywords: Nanoscale zero-valent iron; Bimetallic; Biochar; Chromium; Heavy metal

1. Introduction

Chromium and its compounds are widely used in various fields of industrial production such as electroplating, paints, pigments, printing, and other industries that are indispensable for generating raw materials [1]. There are more than 10,000 electroplating factories in China, and the annual emissions of chromium-containing wastewater are more than 4 billion m^3 [2]. Chromium exists in both the trivalent Cr(III) and the hexavalent Cr(VI) oxidation states; Cr(VI) is highly toxic and easy to accumulate in the body, causing skin, heart and respiratory diseases and other body damage. According to the World Health Organization (WHO) [3], the maximum contaminant level of total chromium in drinking water should not exceed 0.05 mg L^{-1} . Therefore, it is urgent to find effective methods to remove Cr(VI) from water.

Many technologies, including adsorption [4], chemical precipitation [5], ion exchange [6], photocatalysis [7], membrane treatment [8], and reduction [9] were used in the removal of Cr(VI). Among these methods, the reduction of Cr(VI) to Cr(III) by nanoscale zero-valent iron (nZVI) is widely applied and considered an effective method for chromium-contaminated wastewater treatment. nZVI is a very effective agent for removing heavy metals due to its high surface area and reactivity [10,11]. However, nZVI is easily agglomerated and oxidized in some environments, which results in low reactivity [12]. To address these issues, resin [13], activated carbon [14], biochar [15] and other substances [16] have been used as porous-based support materials for the nZVI. In comparison with other materials, biochar has proven to be a cost-effective and environmentally friendly nZVI support due to its large porosity and specific surface area [17].

* Corresponding authors.

Another drawback of nZVI is the formation of iron oxide layers on the surface which decreases its reactivity [18]. It was found that deposition of a second metal such as copper [19], nickel [20] and palladium [21] on the surface can enhance the generation of electrons available to reduce pollutants and increase the activity. Copper (Cu) shows a distinct advantage over other noble metals due to its low cost. In addition, Cu is also one of the essential trace elements for animals and human health [22]. Therefore, copper-iron bimetallic nanoparticles are the preferred choice for nZVI modification when evaluating the cost-effectiveness of water treatment [19,23].

In this study, biochar-supported Cu/Fe bimetallic nanoparticles (Cu-nZVI/BC) were prepared and used to detoxify of Cr(VI) from solutions. The structures of Cu-nZVI/BC were characterized by Brunauer-Emmett-Teller surface area (S_{BET}), transmission electron microscopy (TEM), scanning electron microscopy (SEM) analysis, magnetic, X-ray diffraction (XRD) and X-ray photoelectron spectroscopy (XPS) analyses. The effects of the solution pH, the initial concentration of Cr(VI), the kinetics of Cr(VI) removal, the coexistence of ions and humic acids (HA) were also examined.

2. Materials and methods

2.1. Materials

Ferrous sulfate heptahydrate (99.95% metal basis) and sodium borohydride (98% purity) were purchased from the Shanghai Aladdin Bio-Chem Technology Co., Ltd. (Shanghai, China). Other reagents were provided by the Sinopharm Chemical Reagent Co., Ltd. (Shanghai, China). Biochar was prepared from a herb residue (*Astragalus membranaceus*) at a temperature of 400°C for 2 h under nitrogen.

2.2. Methods

2.2.1. Preparation of Cu-nZVI/BC

The Cu-nZVI/BC were prepared by a borohydride liquid reduction method via the following steps: biochar (2.1 g) was dissolved in 500 mL of a solution containing $\text{FeSO}_4 \cdot 7\text{H}_2\text{O}$ (0.075 mol L^{-1}) and $\text{CuSO}_4 \cdot 5\text{H}_2\text{O}$ (0.003 mol L^{-1}) and stirred vigorously for 4 h under nitrogen. After stirring, NaBH_4 solution (0.6 mol L^{-1} , 500 mL) was added dropwise, which was followed by another 60 min of stirring under nitrogen. The black composite particles were separated from the liquid phase, washed with absolute ethanol and finally vacuum dried at 60°C for 12 h. The water used in this study was bubbled with nitrogen for 2 h before use.

2.2.2. Adsorption experiments

Adsorption experiments were performed using glass bottles (250 mL) at 25°C, and the pH of the solution was adjusted to the required values with 0.1 mol L^{-1} NaOH and 0.1 mol L^{-1} HCl. The effect of solution pH on Cr(VI) (50 mg L^{-1}) adsorption onto Cu-nZVI/BC (0.2 g L^{-1}) was studied (pH: 2.0, 3.0, 4.0, 5.0, 6.0, and 7.0). The effect of the initial Cr(VI) concentration was investigated in the range of 10–125 mg L^{-1} at a pH of 2.0. In addition, the effects of the coexisting ions (Cl^- , NO_3^- and Ca^{2+} , 5 and 10 mmol L^{-1}) and

HA (1, 5, and 10 mg L^{-1}) were studied. The water samples were removed at regular time intervals and filtered through a 0.22 μm filter film. The concentration of Cr(VI) was measured with a 1,5-diphenylcarbazide spectrophotometric method using an ultraviolet spectrophotometer at 540 nm. Experiments in this study were performed in triplicate. The reaction time of all the batch experiments was 240 min.

2.3. Characterizations of Cu-nZVI/BC

The S_{BET} and pore volume (V_{pore}) of Cu-nZVI/BC were calculated by a surface analyzer (QUANTATECH, Auto-sorb-iQA3200-4, USA) with N_2 adsorption. TEM images were obtained by measuring the basic morphology of Cu-nZVI/BC with a JEM 2100F electron microscope at an acceleration voltage of 200 kV. Magnetic properties were determined using a SQUID-VSM vibrating sample magnetometer (Quantum Design, USA). Surface analysis of Cu-nZVI/BC was performed with a monochromatic Al X-ray source at 150 W using XPS (Thermo ESCALAB250Xi, USA). XRD patterns of Cu-nZVI/BC were obtained using an X-ray diffractometer (BRUKER, D8 ADVANCE, Germany) with a high-power Cu K α radioactive source ($\lambda = 0.154$ nm) at 40 kV and 30 mA.

3. Results and discussion

3.1. Characterization of nanoparticles

According to the SEM images (Fig. 1), pores on the surface of the biochar are clearly shown, while there were some agglomerates on the surfaces of the nZVI/BC and

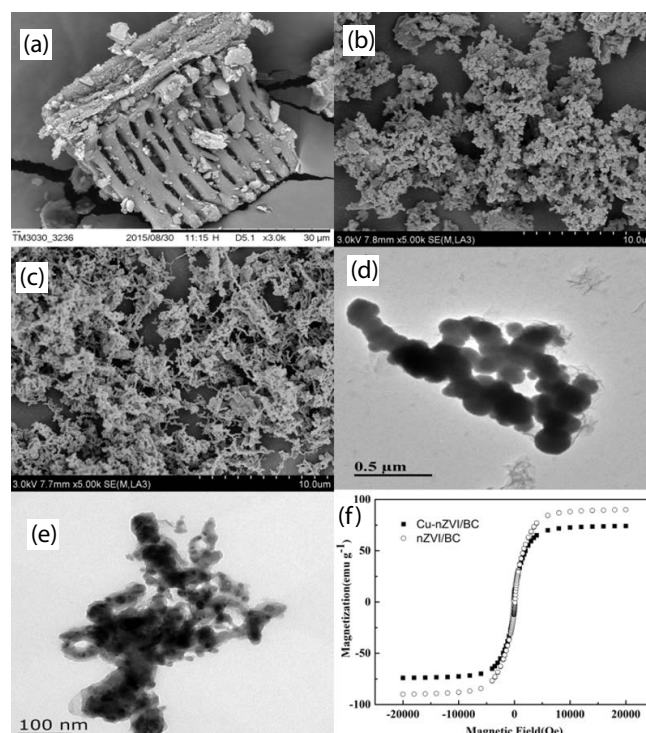


Fig. 1. SEM images of (a) biochar, (b) nZVI/BC, and (c) Cu-nZVI/BC; TEM images of (d) nZVI/BC and (e) Cu-nZVI/BC; (f) Magnetization curve of nanoparticles.

Cu-nZVI/BC. The S_{BET} decreased from 111.48 $\text{m}^2 \text{g}^{-1}$ (biochar) to 59.34 $\text{m}^2 \text{g}^{-1}$ (nZVI/BC) and 26.7 $\text{m}^2 \text{g}^{-1}$ (Cu-nZVI/BC) (Table 1). Previous studies have also shown that the surface area decrease is due to the presence of iron oxides [2] and copper oxides [24], which decrease the surface areas of Cu-nZVI/BC. As shown in the TEM images (Figs. 1d and e), the particle size of Cu-nZVI/BC was in the range of 50–100 nm. The spherical particles may be Fe^0 agglomerates with a layered structure around the Fe core. The specific saturation magnetization (M_s) of nZVI/BC and Cu-nZVI/BC was 89.79 and 73.93 emu g^{-1} (Fig. 1f). The high value of M_s guaranteed a magnetic-separation performance under an external magnetic field, which is an important advantage for the recycling of Cu-nZVI/BC after reaction.

Element mapping analysis (Fig. 2) and XPS survey spectra (Fig. 3a) indicated that Fe, Cu, C and O existed on the surface of Cu-nZVI/BC. In addition, the results of XRD analysis were shown in Fig. 3b. The major peaks were identified as Fe^0 (PDF: 06-0696, $2\theta = 44.5^\circ$), FeOOH (PDF: 34-1226, $2\theta = 26.9^\circ$), Fe_2O_3 (PDF: 25-1402, $2\theta = 20.82^\circ$ and 34.8°), and Fe_3O_4 (PDF: 03-0863, $2\theta = 35.45^\circ$), and the diffraction peaks with $2\theta = 43.4^\circ$ and 50.4° corresponded to copper [19]. The diffraction pattern indicated that the iron oxides and copper oxides were present on the surface of the biochar, and could be attributed to the decrease in surface area. In addition, the characteristic peaks at $2\theta = 43.4^\circ$ and 50.4° (Cu^0) disappeared, and the characteristic peak was identified as Cr_2O_3 (PDF: 03-1124, $2\theta = 54.93^\circ$) after reacting with Cr(VI), indicating the reduction of Cr(VI) to Cr(III) [25].

3.2. Influence of copper modification and solution pH

Fig. 4a shows the removal performance of biochar, nZVI/BC and Cu-nZVI/BC. When BC added, the removal efficiency was 11.64%, indicating the weak ability of biochar to absorb Cr(VI). When combined with the effect of nZVI/BC and Cu-nZVI/BC, the Cr(VI) removal efficiency reached 39.37% and 49.68%, respectively. The results strongly revealed that Cu-nZVI/BC provided better chromium removal ability than nZVI/BC ($p < 0.05$). The reason for this difference may be that copper acted as a catalyst to accelerate the corrosion of nZVI and promoted the removal [26].

The effect of the initial solution pH on Cr(VI) removal is shown in Fig. 4b, and demonstrated that the acidic pH benefited the removal process. The removal efficiency was 50.57% at pH 2.0 (q_e , $126.41 \pm 3.75 \text{ mg g}^{-1}$) and decreased to 43.77% (pH 3.0) and 4.94% (pH 7.0) ($p < 0.05$). Similar results were observed when Fe^0/Cu bimetallic nanoparticles

were used to remove Cr(VI) [27]. Chromium exists in different forms at different pH values (e.g., H_2CrO_4 , HCrO_4^- , $\text{Cr}_2\text{O}_7^{2-}$, CrO_4^{2-}) [28]. When the $\text{pH} < 3$, the predominant Cr(VI) species in solution is HCrO_4^- ; HCrO_4^- converts to $\text{Cr}_2\text{O}_7^{2-}$ and CrO_4^{2-} with an increase in pH [2]. The maximum removal efficiency of Cr(VI) at low pH is mainly due to the adsorption of HCrO_4^- . The adsorption free energy of HCrO_4^- (-2.5 to $-0.6 \text{ kcal mol}^{-1}$) is lower than that of CrO_4^{2-} (-2.1 to $-0.3 \text{ kcal mol}^{-1}$), and consequently, HCrO_4^- is more favorably adsorbed [29].

Moreover, acidic pH could provide cleaner surface of the material and promote decomposition of the surface oxide layer, thus accelerating the corrosion of the copper-iron bimetallic nanoparticles. Exposing surface active sites of Cu-nZVI/BC led to an increase in the removal capacity of Cr(VI). Under alkaline conditions, precipitation was easily produced, which passivated the surface of Cu-nZVI/BC. This process prevented contact between Cu-nZVI/BC and Cr(VI) and thus decreased the removal efficiencies.

3.3. Adsorption isotherm

The removal capacity of Cr(VI) decreased from 100% to 19.04% when its initial concentration increased from 10 to 125 mg L^{-1} (Fig. 5a). This is because the initial Cr(VI) concentration increased and the amount of Cu-nZVI/BC added remained unchanged, resulting in a decrease of adsorption sites on the surface of Cu-nZVI/BC [30].

Langmuir Eq. (1) and Freundlich Eq. (2) models were applied to fit the experimental data, and the results are shown in Fig. 5b:

$$\frac{c_e}{q_e} = \frac{c_e}{q_m} + \frac{1}{q_m K_L} \quad (1)$$

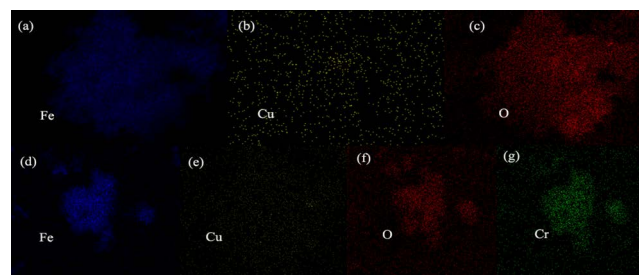


Fig. 2. The elemental mapping images of the Cu-nZVI/BC: (a,b,c) and after reaction:(d, e, f, g).

Table 1
Textural properties of biochar, nZVI and Cu-nZVI/BC

Sample	S_{BET} ($\text{m}^2 \text{g}^{-1}$)	S_{mic} ($\text{m}^2 \text{g}^{-1}$)	V_{Tot} ($\text{cm}^3 \text{g}^{-1}$)	V_{mic} ($\text{cm}^3 \text{g}^{-1}$)	C (%)	Fe (mg g^{-1})	Cu (mg g^{-1})
Biochar	111.48	50.43	0.095	0.0258	57.65	–	–
nZVI/BC	59.34	4.298	0.119	0.0193	17.83	159.41	–
Cu-nZVI/BC	26.7	3.848	0.062	0.0190	12.84	93.425	6.175

S_{mic} : the micropore surface area calculated with the t -plot method

V_{Tot} : total pore volume

V_{mic} : pore volume calculated by using the t -plot method

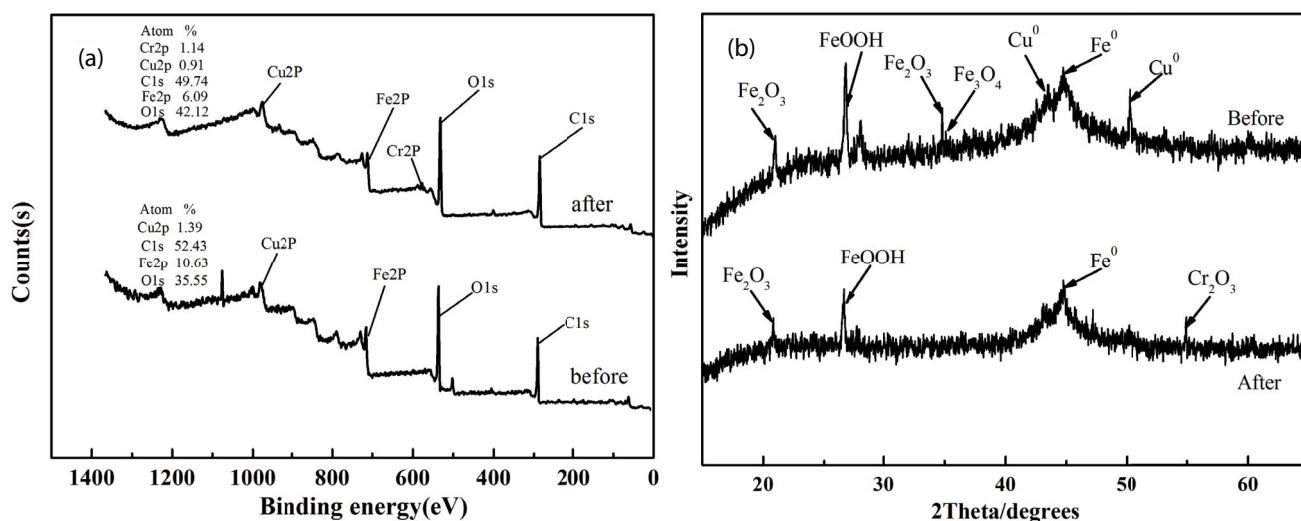


Fig. 3. (a) XPS survey spectra and (b) XRD analysis for Cu-nZVI/BC.

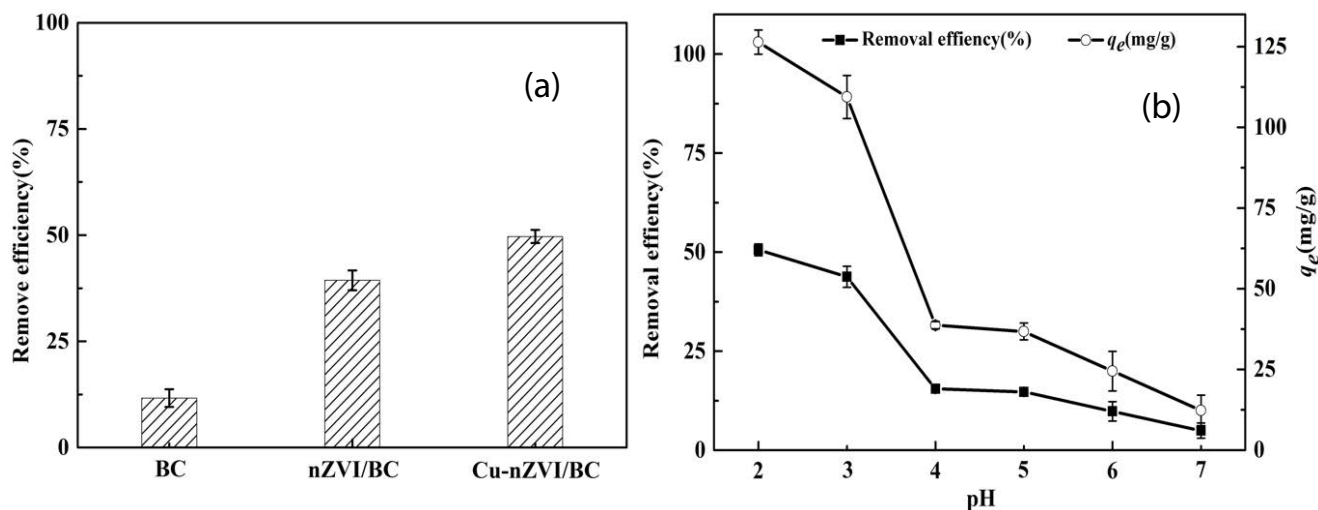


Fig. 4. (a) Removal efficiency of Cr(VI) and (b) the influence of pH on Cr(VI) removal efficiency and adsorption capacity (initial concentration = 50 mg L⁻¹).

$$\log q_e = \log K_f + \frac{1}{n} \log c_e \quad (2)$$

where C_e (mg L⁻¹) is the equilibrium concentration of Cr(VI); q_e (mg g⁻¹) is the Cr(VI) adsorbed capacity at equilibrium; q_m (mg g⁻¹) is the maximum adsorption capacity; K_L (L mg⁻¹) and K_f (mg g⁻¹) (L mg⁻¹)^{1/n} are the Langmuir and Freundlich isotherm constants; and n is a constant related to the affinity between the adsorbent and adsorbate.

The Langmuir isotherm model ($R^2 = 0.998$) yielded a better fit than the Freundlich isotherm model ($R^2 = 0.955$). The Langmuir model assumes that the adsorption occurs on the surface of Cu-nZVI/BC by monolayer adsorption, and the no interaction occurs between pollutant molecules [31]. In addition, the Langmuir model also indicates that adsorption processes are controlled by chemical reactions. The result confirmed that Cu-nZVI/BC have a strong removal efficiency for Cr(VI).

3.4. Adsorption kinetics

In this study, pseudo-first-order (PFO) Eq. (3) and pseudo-second-order kinetic (PSO) Eq. (4) models were used to fit the experimental data, and the results are shown in Figs. 5c and d and Table 2.

$$\ln(q_e - q_t) = \ln q_e - k_1 t \quad (3)$$

$$\frac{t}{q_t} = \frac{1}{k_2 q_e^2} + \frac{t}{q_e} \quad (4)$$

where k_1 (min⁻¹) and k_2 (g mg⁻¹ min⁻¹) are the rate constants for PFO and PSO kinetic models, and q_t and q_e are the Cr(VI) adsorption capacities (mg g⁻¹) at time (t) and at equilibrium.

According to the results, the correlation coefficient values (R^2) of the PSO models were higher than the values of the PFO models. Additionally, the $q_{e,cal}$ values from PSO models were

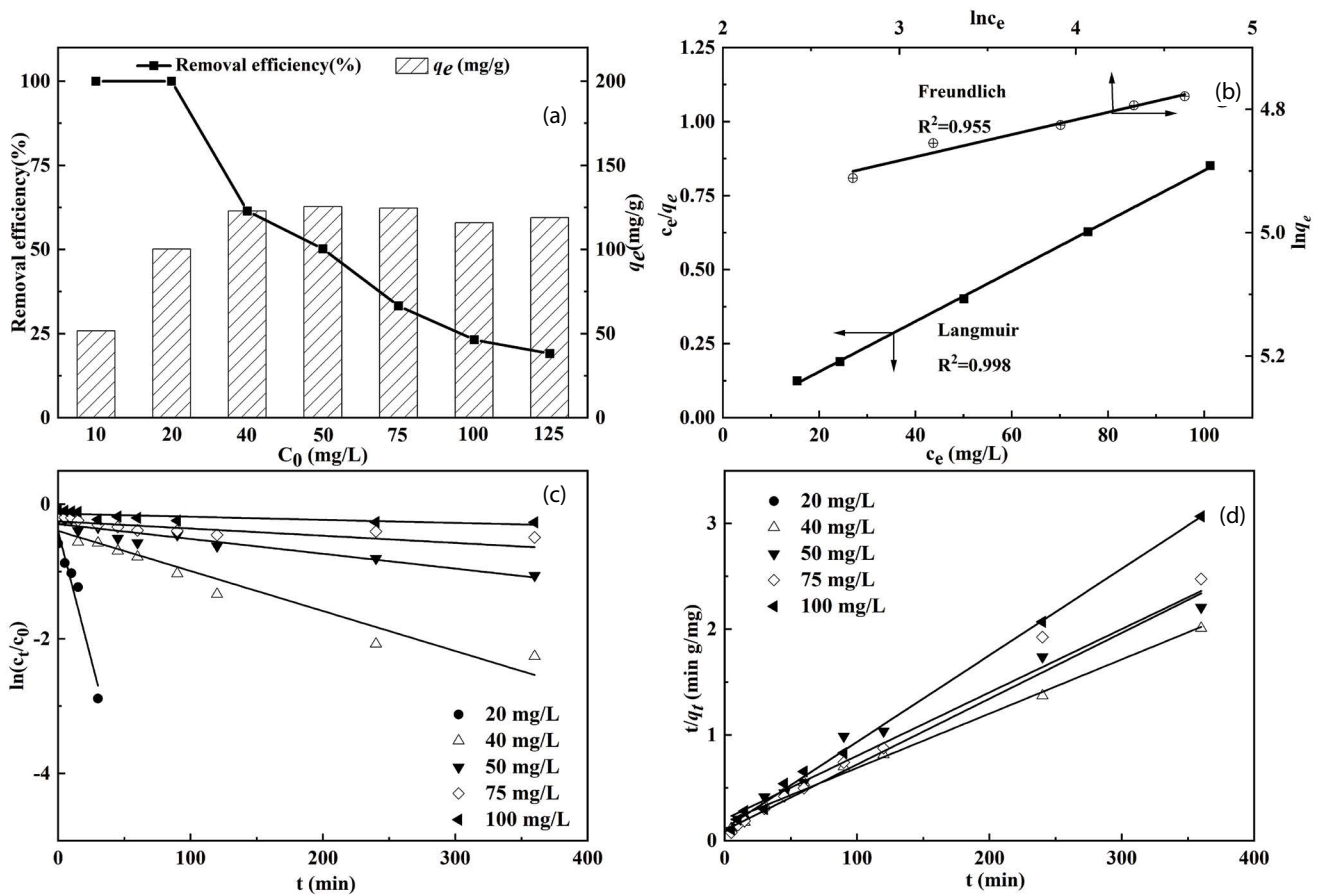


Fig. 5. (a) Effect of initial concentration, (b) equilibrium adsorption isotherms model, (c) pseudo-first-order kinetic, and (d) pseudo-second-order kinetic model of Cr(VI) removal.

Table 2
Kinetic parameters for the adsorption of Cr(VI) onto Cu-nZVI/BC

C_0 (mg L ⁻¹)	q_e (mg g ⁻¹)	Pseudo-first-order kinetics			Pseudo-second-order kinetics		
		$q_{e,cal}$ (mg g ⁻¹)	k_1 (min ⁻¹)	R^2	$q_{e,cal}$ (mg g ⁻¹)	k_2 (g mg ⁻¹ min ⁻¹)	R^2
20	100.33	66.55	0.0763	0.9393	114.94	0.0087	0.9894
40	147.46	107.09	0.0059	0.9346	132.63	0.0051	0.9914
50	137.99	103.86	0.0022	0.8616	142.86	0.006	0.969
75	137.06	114.88	0.0011	0.9473	131.23	0.0069	0.979
100	117.36	83.72	0.0005	0.9656	122.40	0.0082	0.994

closer to the experimental values ($q_{e,exp}$) than the values of the PFO models. These results indicated that the Cr(VI) sorption process follows a PSO mechanism and that the rate-limiting step may be a chemical adsorption process. These results were consistent with previous results. Compared with other materials listed in Table 3, Cu-nZVI/BC demonstrated a good ability for Cr(VI) removal.

3.5. Effect of coexisting ions and HA

As shown in Fig. 6, the influence of coexisting ions (Cl^- , NO_3^- and Ca^{2+}) and HA on the adsorption capacity

Table 3
Adsorption capacities of various some adsorbents for Cr(VI) removal

Materials	pH	C_0 (mg L ⁻¹)	q_e (mg g ⁻¹)	References
Biochar	2.0	100	49.55	[51]
Activated carbon	3.0	100	35.02	[52]
nZVI	3.0	25	17.61	[53]
nZVI/BC	2.0	20	99.98	[54]
Cu-nZVI/BC	2.0	20	100.33	Present work

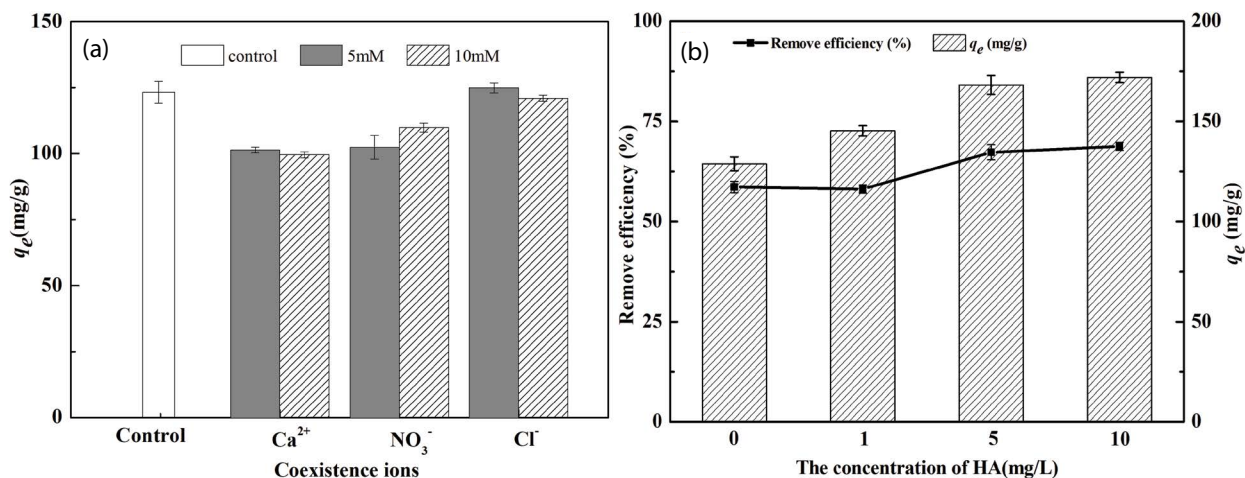


Fig. 6. Effect of (a) coexisting ions and (b) HA on the adsorption capacity of Cu-nZVI/BC for Cr(VI) adsorption.

of Cu-nZVI/BC for Cr(VI) removal over 240 min were investigated. From Fig. 6a, the removal capacity of Cr(VI) decreased from an initial value of $123.20 \pm 4.18 \text{ mg g}^{-1}$ for the control group to $124.91 \pm 1.91 \text{ mg g}^{-1}$ and $121.03 \pm 1.20 \text{ mg g}^{-1}$ when the concentrations of Cl^- were 5 and 10 mM ($p > 0.05$), respectively. The results demonstrated that Cl^- had no obvious influence on Cr(VI) removal compared to the control samples. In contrast to other studies [32,33], NO_3^- inhibited the removal capacity of Cr(VI) in this study (i.e., from $123.20 \pm 4.18 \text{ mg g}^{-1}$ for the control to $102.42 \pm 4.50 \text{ mg g}^{-1}$ with 5 mM NO_3^- and $109.90 \pm 1.65 \text{ mg g}^{-1}$ with 10 mM NO_3^-). These changes could result from NO_3^- oxidizing nZVI to form an oxide layer, leading to the passivation of the material [34]. The removal capacity of Cr(VI) significantly decreased to $101.39 \pm 1.11 \text{ mg g}^{-1}$ and $99.57 \pm 1.17 \text{ mg g}^{-1}$ with addition of 5 and 10 mM Ca^{2+} . The main reason for this difference could be that the presence of Ca^{2+} resulted in nZVI aggregation and thus reduced Cr(VI) removal reactivity [35].

Previous studies have shown that the effect of HA on Cr(VI) removal was inconsistent, including both promotion and inhibition. Zhu et al. [36] found that the presence of HA in aqueous media can inhibit the Cr(VI) removal efficiency. This result might have been due to HA competing with Cr(VI) adsorbed on the active surface sites of nZVI/Cu, thus reducing Cr(VI) removal efficiency. However, the removal efficiency of Cr(VI) was 51.55%, 58.13%, 67.30%, and 68.79% at HA concentrations of HA 0, 1, 5, and 10 mg L^{-1} , respectively ($p < 0.05$). Thus, HA had a promoting effect on the Cr(VI) removal. The underlying reasons might be that (a) HA served as a bridge to stabilize Cu-nZVI/BC particles, thus increasing the removal efficiency of Cr(VI) [37]; (b) HA served to transfer electrons between Cr(VI) and Cu-nZVI/BC, accelerating Cr(VI) removal efficiency [38]; and (c) the negatively charged HA can be adsorbed on the surface of Cu-nZVI/BC, allowing the surface-bound HA to induce a shift from Cr(VI) to Cr(III) [39].

3.6. Mechanism of Cr(VI) removal by Cu-nZVI/BC

To investigate the Cr(VI) removal mechanism, the XPS spectrum of Fe 2p, Cr 2p, and C 1s XPS spectra of the Cu-nZVI/

BC composites before and after reaction with Cr(VI) were obtained (Fig. 7). The C 1s spectrum of fresh Cu-nZVI/BC showed three peaks with binding energies of approximately 284.55, 285.25, and 286.79 eV, which are attributable to the $-\text{CH}_x$, $-\text{C}-\text{O}$ and $\text{O}=\text{C}-\text{O}$, respectively. The intensity of the $\text{O}=\text{C}-\text{O}$ peak at 286.79 eV increased from 17.73% to 24.83% after reaction with Cr(VI). These changes demonstrated that $-\text{C}-\text{O}$ and $\text{O}=\text{C}-\text{O}$ may be involved in chromium removal. These results are in good agreement with other studies [40], which concluded that carboxyl and hydroxyl groups play important roles in heavy metal adsorption.

Additionally, the peaks at 710.7 and 712.6 eV correspond to the binding energies of Fe 2p_{3/2} for Fe(II) and Fe(III), while the peaks at 723.9 and 726.0 eV were assigned to Fe 2p_{1/2} of Fe(II) and Fe(III), respectively [41]; the peaks at 707 eV correspond to Fe^0 [42]. Comparing to the XPS spectra of fresh Cu-nZVI/BC and Cu-nZVI/BC after the reaction with Cr(VI), the fact that the peak of Fe^0 disappeared after reaction can be inferred as a result that Fe^0 was involved in the reaction between Cu-nZVI/BC and Cr(VI). A survey XPS spectrum suggested that Cr(VI) was reduced to Cr(III). The Cr 2p spectra as shown in Fig. 7c after the reaction have two peaks, one at 577.6 eV (Cr 2p_{3/2}) and one at 587.5 eV (Cr 2p_{1/2}) [43]. Montesinos et al. [44] assigned the binding energy at 577.6 eV to Cr oxide [45], while the peak at 587.5 eV corresponded to the binding energies of Cr hydroxide, indicating that co-precipitates were formed during Cr(VI) adsorption and reduction [46]. The XRD results (Fig. 3b) indicated that the presence of Cr_2O_3 on the surface of the material after the reaction, which could indicate that the removal of Cr(VI) by Cu-nZVI/BC was a chemical adsorption process.

The XPS showed that Fe(II) was oxidized and Cr(VI) was reduced to Cr(III) during treatment. The effects of ferrous ions on Cr(VI) removal were studied by the addition of 1,10-phenanthroline and EDTA into the solution. The results showed that the Cr(VI) removal capacity significantly decreased when the 1,10-phenanthroline concentration increased (Fig. 8a). The reason for this may be that 1,10-phenanthroline could form a complexation of Fe(II) that prevented Fe(II) from reducing Cr(VI) [47]. The removal

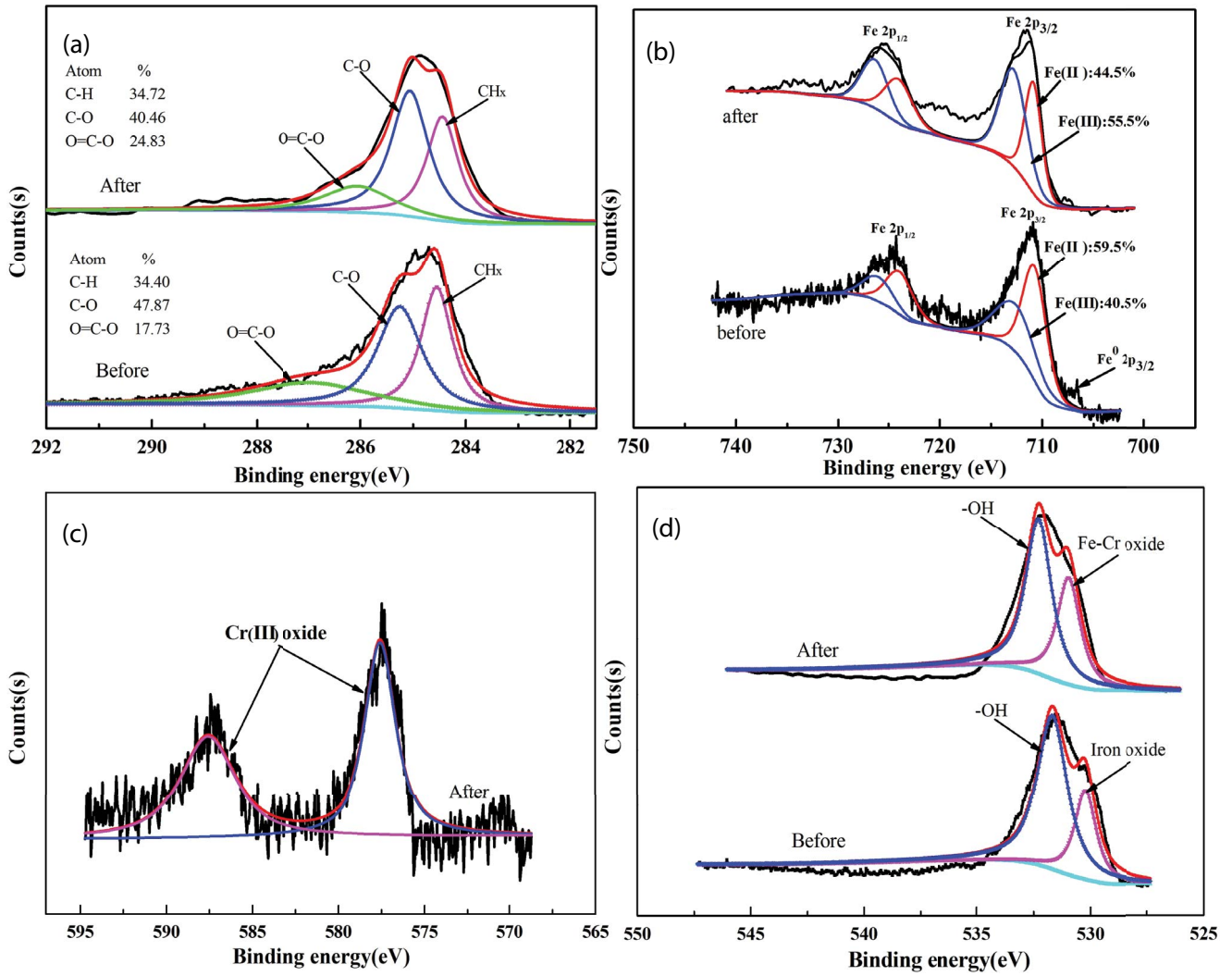


Fig. 7. XPS survey spectra of Cu-nZVI/BC before and after reaction: (a) the C 1s region, (b) the Fe 2p region, (c) the Cr 2p region, and (d) the O 1s region.

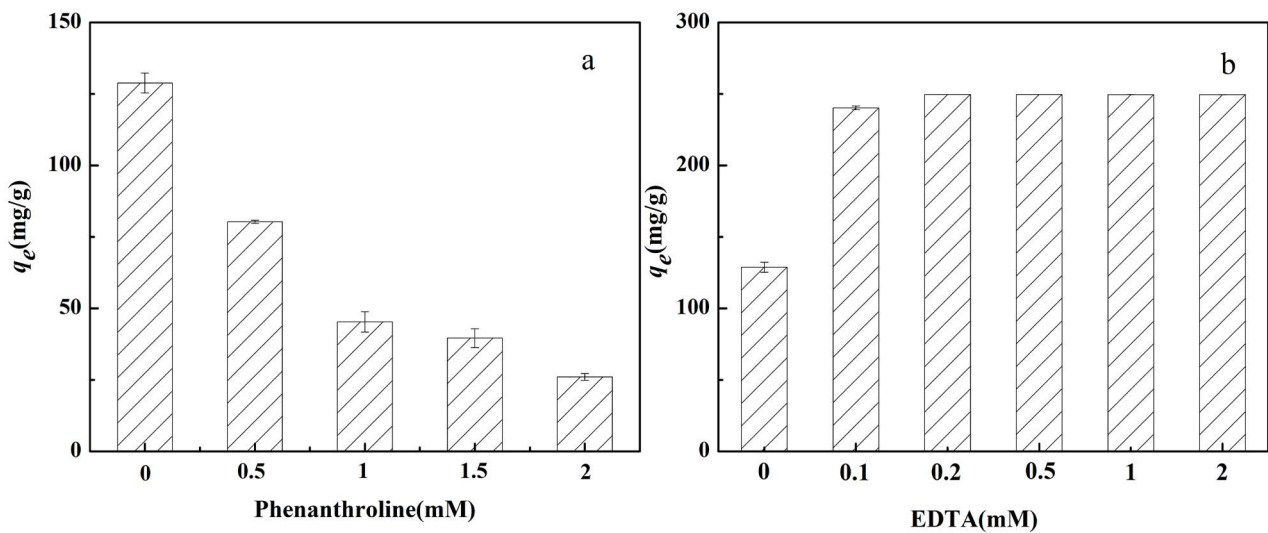


Fig. 8. Effect of (a) Phenanthroline and (b) EDTA on the adsorption capacity of Cu-nZVI/BC for Cr(VI) adsorption.

capacity of Cr(VI) increased from 128 to 250 mg g⁻¹ when EDTA was added to the Cr(VI) solution, which showed that EDTA enhanced Cr(VI) removal (Fig. 8b). EDTA could inhibit precipitation of Fe²⁺/Fe³⁺ and thus decrease passivation on the surface of Cu-nZVI/BC [48], which may be the reason for the increasing removal capacities of Cr(VI) [49]. The above results proved that Fe²⁺ has a crucial contribution to the removal of Cr(VI) [50].

4. Conclusions

In the present research, biochar supported Fe/Cu bimetallic nanoparticles were prepared, characterized and used for Cr(VI) removal experiments. The removal efficiency of Cu-nZVI/BC was investigated based on different influencing factors, including the pH, the initial concentration of Cr(VI), the coexisting ions and HA. The performance of Cu-nZVI/BC in removing Cr(VI) was highly dependent on pH, and the maximum q_m occurred at pH 2. The experimental data followed the PSO model, and the Langmuir isotherm model was the best-fitting isotherm model. Coexisting ions (Cl⁻, NO₃⁻ and Ca²⁺) inhibited Cr(VI) removal, while HA promoted Cr(VI) removal. Reduction of Cr(VI) to Cr(III) and chemical adsorption of Cr(VI) were the possible mechanisms for the interaction between Cu-nZVI/BC and Cr(VI). Cu-nZVI/BC prepared with low-cost herb-residue is an efficient and environmentally friendly detoxification material for Cr(VI) detoxification in wastewater.

Acknowledgements

This work was supported by the Natural Science Foundation of Jiangsu Province (CN) (BK20150693), the National Natural Science Foundation of China (NSFC, 201707166), College Students Innovation Project for the R&D of Novel Drugs (NO. J1310032) and Fundamental Research Funds for the Central Universities (No. 2632018FY01).

References

- R. Saha, R. Nandi, B. Saha, Sources and toxicity of hexavalent chromium, *J. Coord. Chem.*, 64 (2011) 1782–1806.
- S.-y. Wang, Y.-k. Tang, K. Li, Y.-y. Mo, H.-f. Li, Z.-q. Gu, Combined performance of biochar sorption and magnetic separation processes for treatment of chromium-contained electroplating wastewater, *Bioresour. Technol.*, 174 (2014) 67–73.
- Guidelines for Drinking Water Quality, WHO, 2011, pp. 104–108.
- R. Karthik, S. Meenakshi, Removal of Cr(VI) ions by adsorption onto sodium alginate-polyaniline nanofibers, *Int. J. Biol. Macromol.*, 72 (2015) 711–717.
- M.A. Behnajady, S. Bimeghdar, Synthesis of mesoporous NiO nanoparticles and their application in the adsorption of Cr(VI), *Chem. Eng. J.*, 239 (2014) 105–113.
- R.S. Azarudeen, R. Subha, D. Jeyakumar, A.R. Burkanudeen, Batch separation studies for the removal of heavy metal ions using a chelating terpolymer: synthesis, characterization and isotherm models, *Sep. Purif. Technol.*, 116 (2013) 366–377.
- W. Liu, J. Ni, X. Yin, Synergy of photocatalysis and adsorption for simultaneous removal of Cr(VI) and Cr(III) with TiO₂ and titanate nanotubes, *Water Res.*, 53 (2014) 12–25.
- H.-m. Xu, J.-f. Wei, X.-l. Wang, Nanofiltration hollow fiber membranes with high charge density prepared by simultaneous electron beam radiation-induced graft polymerization for removal of Cr(VI), *Desalination*, 346 (2014) 122–130.
- C. Ding, W. Cheng, Y. Sun, X. Wang, Effects of *Bacillus subtilis* on the reduction of U(VI) by nano-Fe⁰, *Geochim. Cosmochim. Acta*, 165 (2015) 86–107.
- Y. Su, A.S. Adeleye, A.A. Keller, Y. Huang, C. Dai, X. Zhou, Y. Zhang, Magnetic sulfide-modified nanoscale zerovalent iron (S-nZVI) for dissolved metal ion removal, *Water Res.*, 74 (2015) 47–57.
- Y. Zou, X. Wang, A. Khan, P. Wang, Y. Liu, A. Alsaedi, T. Hayat, X. Wang, Environmental remediation and application of nanoscale zero-valent iron and its composites for the removal of heavy metal ions: a review, *Environ. Sci. Technol.*, 50 (2016) 7290–7304.
- H. Chen, H. Luo, Y. Lan, T. Dong, B. Hu, Y. Wang, Removal of tetracycline from aqueous solutions using polyvinylpyrrolidone (PVP-K30) modified nanoscale zero valent iron, *J. Hazard. Mater.*, 192 (2011) 44–53.
- F. Fu, D.D. Dionysiou, H. Liu, The use of zero-valent iron for groundwater remediation and wastewater treatment: a review, *J. Hazard. Mater.*, 267 (2014) 194–205.
- A.M.E. Khalil, O. Eljamal, T.W.M. Amen, Y. Sugihara, N. Matsunaga, Optimized nano-scale zero-valent iron supported on treated activated carbon for enhanced nitrate and phosphate removal from water, *Chem. Eng. J.*, 309 (2017) 349–365.
- J. Yan, L. Han, W. Gao, S. Xue, M. Chen, Biochar supported nanoscale zerovalent iron composite used as persulfate activator for removing trichloroethylene, *Bioresour. Technol.*, 175 (2015) 269–274.
- X. Fei, L. Cao, L. Zhou, Y. Gu, X. Wang, Degradation of bromamine acid by nanoscale zero-valent iron (nZVI) supported on sepiolite, *Water Sci. Technol.*, 66 (2012) 2539–2545.
- J. Shang, J. Pi, M. Zong, Y. Wang, W. Li, Q. Liao, Chromium removal using magnetic biochar derived from herb-residue, *J. Taiwan Inst. Chem. Eng.*, 68 (2016) 289–294.
- F. Zhu, S. He, T. Liu, Effect of pH, temperature and co-existing anions on the Removal of Cr(VI) in groundwater by green synthesized nZVI/Ni, *Ecotoxicol. Environ. Saf.*, 163 (2018) 544–550.
- B. Lai, Y. Zhang, Z. Chen, P. Yang, Y. Zhou, J. Wang, Removal of *p*-nitrophenol (PNP) in aqueous solution by the micron-scale iron-copper (Fe/Cu) bimetallic particles, *Appl. Catal., B*, 144 (2014) 816–830.
- X. Zhou, G. Jing, B. Lv, Z. Zhou, R. Zhu, Highly efficient removal of chromium(VI) by Fe/Ni bimetallic nanoparticles in an ultrasound-assisted system, *Chemosphere*, 160 (2016) 332–341.
- Y. Gao, F. Wang, Y. Wu, R. Naidu, Z. Chen, Comparison of degradation mechanisms of microcystin-LR using nanoscale zero-valent iron (nZVI) and bimetallic Fe/Ni and Fe/Pd nanoparticles, *Chem. Eng. J.*, 285 (2016) 459–466.
- K.O. Soetan, C.O. Olaiya, O.E. Oyewole, The importance of mineral elements for humans, domestic animals and plants: a review, *Afr. J. food Sci.*, 4 (2010) 200–222.
- Z. Xiong, B. Lai, P. Yang, Y. Zhou, J. Wang, S. Fang, Comparative study on the reactivity of Fe/Cu bimetallic particles and zero valent iron (ZVI) under different conditions of N₂, air or without aeration, *J. Hazard. Mater.*, 297 (2015) 261–268.
- R. Yamaguchi, S. Kurosu, M. Suzuki, Y. Kawase, Hydroxyl radical generation by zero-valent iron/Cu (ZVI/Cu) bimetallic catalyst in wastewater treatment: heterogeneous Fenton/Fenton-like reactions by Fenton reagents formed in-situ under oxic conditions, *Chem. Eng. J.*, 334 (2018) 1537–1549.
- S.-S. Chen, B.-C. Hsu, L.-W. Hung, Chromate reduction by waste iron from electroplating wastewater using plug flow reactor, *J. Hazard. Mater.*, 152 (2008) 1092–1097.
- M. Rivero-Huguet, W.D. Marshall, Reduction of hexavalent chromium mediated by micro- and nano-sized mixed metallic particles, *J. Hazard. Mater.*, 169 (2009) 1081–1087.
- F. Zhu, L. Li, S. Ma, Z. Shang, Effect factors, kinetics and thermodynamics of remediation in the chromium contaminated soils by nanoscale zero valent Fe/Cu bimetallic particles, *Chem. Eng. J.*, 302 (2016) 663–669.
- V.K. Gupta, D. Pathania, S. Agarwal, S. Sharma, Removal of Cr(VI) onto *Ficus carica* biosorbent from water, *Environ. Sci. Pollut. Res.*, 20 (2013) 2632–2644.

- [29] P. Yuan, M. Fan, D. Yang, H. He, D. Liu, A. Yuan, J. Zhu, T. Chen, Montmorillonite-supported magnetite nanoparticles for the removal of hexavalent chromium [Cr(VI)] from aqueous solutions, *J. Hazard. Mater.*, 166 (2009) 821–829.
- [30] U.K. Garg, M.P. Kaur, V.K. Garg, D. Sud, Removal of hexavalent chromium from aqueous solution by agricultural waste biomass, *J. Hazard. Mater.*, 140 (2007) 60–68.
- [31] X. Lv, X. Xue, G. Jiang, D. Wu, T. Sheng, H. Zhou, X. Xu, Nanoscale zero-valent iron (nZVI) assembled on magnetic Fe₃O₄/graphene for chromium (VI) removal from aqueous solution, *J. Colloid Interface Sci.*, 417 (2014) 51–59.
- [32] F. Zhu, L. Li, W. Ren, X. Deng, T. Liu, Effect of pH, temperature, humic acid and coexisting anions on reduction of Cr(VI) in the soil leachate by nZVI/Ni bimetal material, *Environ. Pollut.*, 227 (2017) 444–450.
- [33] R. Fu, X. Zhang, Z. Xu, X. Guo, D. Bi, W. Zhang, Fast and highly efficient removal of chromium (VI) using humus-supported nanoscale zero-valent iron: influencing factors, kinetics and mechanism, *Sep. Purif. Technol.*, 174 (2017) 362–371.
- [34] C. Dai, Z. Zhou, X. Zhou, Y. Zhang, Removal of Sb(III) and Sb(V) from aqueous solutions using nZVI, *Water Air Soil Pollut.*, 225 (2014) 1799.
- [35] M. Basnet, A. Gershanov, K.J. Wilkinson, S. Ghoshal, N. Tufenkji, Interaction between palladium-doped zerovalent iron nanoparticles and biofilm in granular porous media: characterization, transport and viability, *Environ. Sci.: Nano*, 3 (2016) 127–137.
- [36] F. Zhu, S. Ma, T. Liu, X. Deng, Green synthesis of nano zero-valent iron/Cu by green tea to remove hexavalent chromium from groundwater, *J. Cleaner Prod.*, 174 (2018) 184–190.
- [37] W.-W. Tang, G.-M. Zeng, J.-L. Gong, J. Liang, P. Xu, C. Zhang, B.-B. Huang, Impact of humic/fulvic acid on the removal of heavy metals from aqueous solutions using nanomaterials: a review, *Sci. Total Environ.*, 468 (2014) 1014–1027.
- [38] X. Lv, Y. Hu, J. Tang, T. Sheng, G. Jiang, X. Xu, Effects of co-existing ions and natural organic matter on removal of chromium (VI) from aqueous solution by nanoscale zero valent iron (nZVI)-Fe₃O₄ nanocomposites, *Chem. Eng. J.*, 218 (2013) 55–64.
- [39] Y.-J. Zhang, J.-L. Ou, Z.-K. Duan, Z.-J. Xing, Y. Wang, Adsorption of Cr(VI) on bamboo bark-based activated carbon in the absence and presence of humic acid, *Colloids Surf., A*, 481 (2015) 108–116.
- [40] X. Dong, L.Q. Ma, Y. Li, Characteristics and mechanisms of hexavalent chromium removal by biochar from sugar beet tailing, *J. Hazard. Mater.*, 190 (2011) 909–915.
- [41] J. Lin, M. Sun, X. Liu, Z. Chen, Functional kaolin supported nanoscale zero-valent iron as a Fenton-like catalyst for the degradation of Direct Black G, *Chemosphere*, 184 (2017) 664–672.
- [42] L. Qian, X. Shang, B. Zhang, W. Zhang, A. Su, Y. Chen, D. Ouyang, L. Han, J. Yan, M. Chen, Enhanced removal of Cr(VI) by silicon rich biochar-supported nanoscale zero-valent iron, *Chemosphere*, 215 (2019) 739–745.
- [43] B.A. Manning, J.R. Kiser, H. Kwon, S.R. Kanel, Spectroscopic investigation of Cr(III)- and Cr(VI)-treated nanoscale zerovalent iron, *Environ. Sci. Technol.*, 41 (2007) 586–592.
- [44] V.N. Montesinos, N. Quici, E.B. Halac, A.G. Leyva, G. Custo, S. Bengio, G. Zampieri, M.I. Litter, Highly efficient removal of Cr(VI) from water with nanoparticulated zerovalent iron: understanding the Fe(III)–Cr(III) passive outer layer structure, *Chem. Eng. J.*, 244 (2014) 569–575.
- [45] S. Zhang, H. Lyu, J. Tang, B. Song, M. Zhen, X. Liu, A novel biochar supported CMC stabilized nano zero-valent iron composite for hexavalent chromium removal from water, *Chemosphere*, 217 (2019) 696–694.
- [46] X. Tian, W. Wang, N. Tian, C. Zhou, C. Yang, S. Komarneni, Cr(VI) reduction and immobilization by novel carbonaceous modified magnetic Fe₃O₄/halloysite nanohybrid, *J. Hazard. Mater.*, 309 (2016) 151–156.
- [47] Q. Shao, C. Xu, Y. Wang, S. Huang, B. Zhang, L. Huang, D. Fan, P.G. Tratnyek, Dynamic interactions between sulfidated zerovalent iron and dissolved oxygen: mechanistic insights for enhanced chromate removal, *Water Res.*, 135 (2018) 322–330.
- [48] T. Yang, L. Meng, S. Han, J. Hou, S. Wang, X. Wang, Simultaneous reductive and sorptive removal of Cr(VI) by activated carbon supported β-FeOOH, *RSC Adv.*, 7 (2017) 34687–34693.
- [49] H. Dong, Q. He, G. Zeng, L. Tang, L. Zhang, Y. Xie, Y. Zeng, F. Zhao, Degradation of trichloroethene by nanoscale zero-valent iron (nZVI) and nZVI activated persulfate in the absence and presence of EDTA, *Chem. Eng. J.*, 316 (2017) 410–418.
- [50] L. Huang, S. Zhou, F. Jin, J. Huang, N. Bao, Characterization and mechanism analysis of activated carbon fiber felt-stabilized nanoscale zero-valent iron for the removal of Cr(VI) from aqueous solution, *Colloids Surf., A*, 447 (2014) 59–66.
- [51] L. Zhou, Y. Liu, S. Liu, Y. Yin, G. Zeng, X. Tan, X. Hu, X. Hu, L. Jiang, Y. Ding, S. Liu, X. Huang, Investigation of the adsorption-reduction mechanisms of hexavalent chromium by ramie biochars of different pyrolytic temperatures, *Bioresour. Technol.*, 218 (2016) 351–359.
- [52] J. Yang, M. Yu, W. Chen, Adsorption of hexavalent chromium from aqueous solution by activated carbon prepared from longan seed: kinetics, equilibrium and thermodynamics, *J. Ind. Eng. Chem.*, 21 (2015) 414–422.
- [53] S. Zhou, Y. Li, J. Chen, Z. Liu, Z. Wang, P. Na, Enhanced Cr(VI) removal from aqueous solutions using Ni/Fe bimetallic nanoparticles: characterization, kinetics and mechanism, *RSC Adv.*, 4 (2014) 50699–50707.
- [54] J. Shang, M. Zong, Y. Yu, X. Kong, Q. Du, Q. Liao, Removal of chromium (VI) from water using nanoscale zerovalent iron particles supported on herb-residue biochar, *J. Environ. Manage.*, 197 (2017) 331–337.